

# Breathing Pattern Detection Using Narrow Sweep Band mmWave FMCW Radar

**Abstract**—Accurate classification and detection of breathing patterns are critical for detecting respiratory disorders, managing health conditions, and enabling timely interventions. Traditional methods hinge on clinical settings, specialized equipment, and professional oversight, limiting their wide deployment and real-time use in contemporary healthcare including home care and self-care. Existing wireless methods utilize millimeter Wave (mmWave) frequency-modulated continuous wave (FMCW) radar sensing to automatically detect respiratory patterns, enabling contactless personal health monitoring without privacy intrusion. However, state-of-the-art (SOTA) solutions utilize dedicated high-frequency radar equipments and consequently sacrifice compatibility with communication requirements. This paper proposes a breathing detection scheme based on mmWave FMCW radar technique at 28 GHz. Different from SOTA solutions, our design achieves accurate detection using only 2 MHz bandwidth, meeting both communication and sensing requirements for in-home health monitoring applications without the need for additional hardware beyond standard communication devices. Experimentation on the USRP platform demonstrates the effectiveness of our design. Using CNN for feature extraction, we can achieve a detection accuracy of 90% which is arguably comparable to SOTA.

**Index Terms**—Integrated Sensing and Communication (ISAC), mmWave Sensing, mmWave FMCW Radar, Machine Learning, Spectrum Sensing, Respiration Detection

## I. INTRODUCTION

Respiration is one of the most vital human life activities and plays a critical role in maintaining normal physiological and mental functions and health. Key respiratory parameters provide valuable insights into an individual's physical and psychological states. Therefore, accurate and timely detection of respiration disorders is not only significant but also deserves greater attention. In the past decades, many mature respiration detection technologies have been used, including Capnography [1], Pulse Oximetry [2], Arterial Blood Gas (ABG) Analysis [3], and Magnetic Resonance Imaging (MRI) of lungs [4]. However, these methods typically require specialized equipments that can only be used in hospitals or dedicated facilities by trained professionals, which limits their wide accessibility. With the trend of telehealth and in-home health and wellness, there is a pertinent need for converting such health monitoring into daily use at home. To this end, one requirement is to design portable wearable medical sensors or re-purpose general-purpose personal devices (e.g., smart phones) for such health monitoring. For example, Respiratory Inductive Plethysmography (RIP) [5] places sensors around the chest and abdomen to measure the volume changes associated with breathing. The other requirement is to allow automatic respiration disorder detection considering health professionals

are not always available when urgent interventions are needed at home. To meet these requirements, an urgent need exists for a system capable of unobtrusively and automatically monitoring and recognizing abnormal breathing patterns across various scenarios without constant human supervision.

Tan et al. [6] proposed a vision-based contactless method for monitoring respiration rate. It relies on processing videos or images captured by cameras, such as video cameras, infrared thermal cameras, depth cameras, etc [7]. This method depends on camera quality, and is vulnerable to environmental changes (e.g., lighting conditions, temperature, camera angle, and object blocking). Due to the camera captured and image processing, it also raises privacy concerns and increases high-computing complexity.

In addition to necessary contactless requirements, the respiration monitoring system must integrate communication capabilities to detect respiratory abnormalities in real-time and upload respiratory data reports to family practices or hospital facilities, enabling timely diagnosis and intervention to prevent missed treatment opportunities. *Integrated Sensing and Communication* (ISAC) [8] is an emerging paradigm that combines wireless communication and sensing functionalities within the same system. ISAC leverages shared hardware and spectral resources to enable simultaneous communication and sensing, which can meet timely respiration monitoring and results uploading.

Several literatures parallelly focus on RF-based sensing methods (e.g., WiFi, RFID, and radar), which compensate the deficiencies of vision-based methods leveraging ISAC. WiFi sensing detect chest movements during breathing by observing signal variations, i.e., Channel State Information. Liu et al. [9] used CSI to detect respiration rate during sleep with WiFi and access point (AP) pairs. Qiu et al. [10] proposed a method of combining multiple WiFi channels to increase signal bandwidth utilizing CSI. RFID sensing methods utilize the Received Signal Strength Indicator (RSSI) to achieve respiratory monitoring [11][12]. However, the lower frequency bands of WiFi and RFID signals reduce the sensitivity to fine respiratory motions and are affected by environmental easily.

In contrast, radars operating at higher frequencies (e.g., continuous wave (CW) Doppler radar [13][14][15], ultra-wideband (UWB) radar [16][17]) have fine resolutions. Although these techniques are capable of detecting slight chest movements, they usually consume a high transmission power and are less applicable for real-time monitoring especially in home settings. Frequency-modulated continuous wave (FMCW) radar, on the other hand, offers low power

consumption, real-time, and contactless measurement while maintaining a high resolution. It features a simple transceiver architecture, operates over a wide frequency range, and has a low sampling rate requirement. Additionally, FMCW radar simplifies proximity detection, and tolerates obstructing objects, making it exceptionally suited for breathing vibration detection [18][19][20]. Therefore, recent researches take advantage of FMCW at millimeter wave (mmWave) frequencies for breathing detection.

Alizadeh et al. [21] proposed a scheme using 77 GHz FMCW radar with 3.99 GHz sweep bandwidth to extract the respiration and heart rate. Herein, Li et al. [22] decreased FMCW radar sweep bandwidth to 896 MHz bandwidth to identify and localize a stationary human in NLOS regions by combining NLOS object detection with vital sign monitoring. Furthermore, Wang et al. [23] monitored both respiratory rate and heartbeat rate with lower sweep bandwidth, i.e., 72 MHz. These works use signal processing techniques to achieve high detection accuracy. Hao et al. [24] developed an image processing scheme to accurately classify four breathing patterns achieving an overall accuracy of 94.75% by using HOG support vector machine (G-SVM). Wang et al. [25] extracted statistical features for classification using (SVM) and K-nearest neighbor (KNN), and the accuracy was 98.25% and 88.75%, respectively. Despite of high accuracies, these studies use specific radar hardware for high-frequency millimeter-wave radar (76-81 GHz) to ensure high-precision detection. At such high frequencies, achieving stable and reliable communication remains a significant challenge, making them unsuitable for ISAC systems, which require simultaneous support for communication and sensing.

To address this challenge, we consider a system that operates at 28 GHz, a frequency that has been proven to support reliable communication while enabling high-precision detection. This dual capability makes 28 GHz an ideal candidate for ISAC systems. Under this setup, maintaining communication quality is critical, which necessitates careful allocation of communication resources. To avoid excessive resource consumption for radar sensing, we design a FMCW radar breathing detection scheme using a narrow sweep bandwidth of 2 MHz to achieve breathing patterns detection. The narrow bandwidth minimizes the impact on communication resources while reducing computational complexity, power consumption, and implementation costs, making the design efficient and practical for in-home health monitoring applications. We use Support Vector Machines Classification (SVM-C), Long Short Term Memory (LSTM), Convolutional Neural Network (CNN), and combined LSTM with CNN (LSTM+CNN) for classification, realizing the recognition of different breathing patterns. Our contributions are as follows:

- We propose a narrow bandwidth contactless 28 GHz mmWave FMCW radar breathing detection scheme. Different from previous solutions, our design utilizes a narrow sweep bandwidth of 2 MHz and a stable communication frequency of 28 GHz.
- Our design functions with standard mmWave communica-

cation devices without requiring any additional hardware for sensing.

- We detect respiratory patterns across a frequency range instead of assuming a fixed respiratory frequency.
- Extensive experiments on the USRP device and mmWave antennas validate the effectiveness of our design. Using CNN for feature extraction, we can achieve a detection accuracy of 90% which is arguably comparable to SOTA.

The rest of the paper is organized as follows. Section II describes technical preliminaries. Our breathing patterns detection scheme is elaborated in Section III. The experimental evaluations are illustrated in Section IV. Section V concludes this paper.

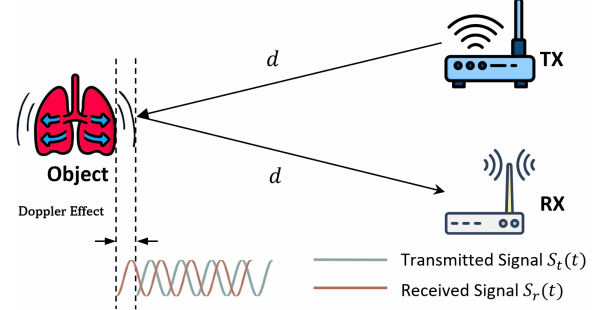


**Figure 1:** The signal emitted from TX towards a subject exhibiting the Doppler effect, and reflected back to RX.

## II. TECHNICAL PRELIMINARIES

We first briefly introduce an FMCW signal commonly used in existing works. Subsequently, we provide some insights into three different breathing patterns.

### A. FMCW

Frequency Modulated Continuous Wave (FMCW) is a radar modulation technique where the frequency of a continuous wave signal varies over time. As shown in Fig. 1, a transmitted FMCW signal  $S_t(t)$  is sent to the breathing subject and expressed as:

$$S_t(t) = A \cos(2\pi(f_c t + \frac{B}{2T} t^2)) \quad (1)$$

where  $A$  is the amplitude,  $f_c$  is the carrier frequency,  $B$  is the sweep bandwidth, and  $T$  is the chirp duration. By calculating the rate of change of the phase of the transmitted signal, the instantaneous transmitted frequency  $f_t(t)$  equals to:

$$f_t(t) = \frac{1}{2\pi} \frac{d}{dt}(2\pi(f_c t + \frac{B}{2T} t^2)) = f_c + \frac{B}{T} t \quad (2)$$

From eq. 2 can observe the chirp characteristic of FMCW radar signal, where the frequency changes linearly over time within a fixed range. This variation in frequency enables the radar to simultaneously determine the range and velocity of the subject. When reflecting off from the subject, the signal will experience a time delay  $\tau = \frac{2d}{c}$ , where  $c$  is the speed of light and  $2d$  represents the total traveling path of  $S_t(t)$  from TX to the subject and reflected back to RX. Since the distance between TX and the subject is identical to the distance between

the subject and RX. With this time delay, the received signal  $S_r(t)$ , is then given by:

$$S_r(t) = A \cos(2\pi(f_c(t - \tau) + \frac{B}{2T}(t - \tau)^2)) \quad (3)$$

According to eq. 3, the transmitted signal continues to sweep linearly in frequency throughout the process. The instantaneous received frequency  $f_r(t)$  expressed as:

$$\begin{aligned} f_r(t) &= \frac{1}{2\pi} \frac{d}{dt} (2\pi(f_c(t - \tau) + \frac{B}{2T}(t - \tau)^2)) \\ &= f_c + \frac{B}{T}(t - \tau) \end{aligned} \quad (4)$$

While the transmitted signal continuous to sweep in frequency during the round-trip travel time ( $\tau$ ), the received signal delayed by  $\tau$  has a frequency corresponding to an earlier time in the chirp. The difference between the instantaneous transmitted frequency  $f_t(t)$  and received frequency  $f_r(t)$  is called beat frequency  $f_b$ :

$$f_b = f_t(t) - f_r(t) = \frac{2Bd}{cT} \quad (5)$$

For periodic chest motions due to breathing, a dynamic component  $f_D$  caused by the periodic Doppler effect will be added to beat frequency  $f_b$ . The  $f_D = A \sin(2\pi f_{breath} t)$ , where  $A$  is the amplitude of the frequency modulation caused by the chest as it moves and  $f_{breath}$  is the breathing frequency. In this moving subjects scenario, we get the moving subjects beat frequency  $f_{mb}$  as the follow:

$$f_{mb} = f_D + \frac{2Bd}{cT} \quad (6)$$

The reason for calculating the beat frequency is that during inhalation and exhalation, the chest movement cause a slight change in the range. The periodic motion modulates the beat frequency over time. By performing Fast Fourier Transform (FFT) on this modulated beat frequency  $f_{mb}$ , the static component  $\frac{2Bd}{cT}$  appears as the peak at 0 Hz and the dynamic component  $f_D$  will produce a peak that corresponds to breathing frequency.

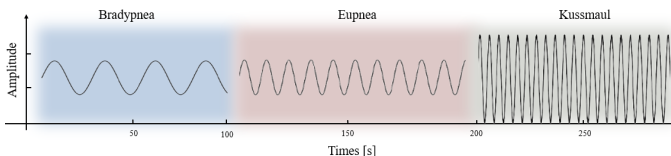


**Figure 2:** Waveform examples for three different breathing patterns: Bradypnea, Eupnea, and Kussmaul.

### B. Breathing Patterns

There are numerous pathological conditions associated with breathing functions, each characterized by unique patterns of breathing that reflect underlying physiological or pathological states. In this paper, we focus on three distinctive breathing patterns, Bradypnea, Eupnea, and Kussmaul breathing [26]. Normal breathing, also known as Eupnea, reflects smooth and rhythmic movements of the chest and diaphragm. Bradypnea represents abnormally slow breathing, often resulting from

hypoventilation caused by drug overdoses, brainstem injury, or metabolic disorders. In contrast to this, Kussmaul breathing is a form of hyperventilation that occurs in metabolic acidosis, such as diabetic ketoacidosis [27][28][29]. Fig. 2 shows a visual representation of the breathing patterns.

**Table I: BREATHING PATTERNS DESCRIPTION**

NO.	PATTERNS	RESPIRATION EFFORT	RESPIRATORY RATE RANGE BREATHS PER MINUTE
1	Bradypnea	1	5-10
2	Eupnea	1	12-25
3	Kussmaul	2.5	20-35

The key aspects to distinguish these patterns are Respiratory Rate (RR) and Respiratory Effort (RE). RR refers to the number of breaths a person takes per minute. This key sign is used to assess a person's breathing efficiency and overall respiratory function. RE, on the other hand, refers to energy expended by the respiratory muscles to inhale and exhale. It reflects the degree of difficulty of breathing. RE isn't quantified in standardized units, it is often rated using biomechanical metrics in research settings. As shown in table I, in healthy conditions such as Eupnea, the RR is 12-25 breaths per minute with a minimal breathing effort level rated as 1. Though with the same effort level, Bradypnea's breathing rate decreases to 5-10 breaths per minute. Kussmaul breathing, featuring a rapid and deep breathing pattern, has a RR of 20-35 breaths per minute and a RE significantly higher, rated as 2.5.

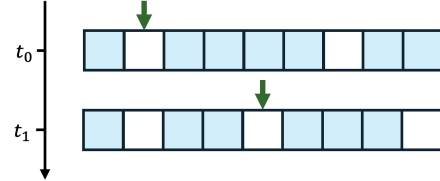


**Figure 3:** Spectrum sensing example over time. White space means idle resource blocks, blue space means occupied.

## III. OUR DESIGN

This section first discusses the preliminaries of spectrum sensing. Then we present our technique for detecting breathing patterns. We also describe the machine learning algorithms we used.

### A. Preliminaries of Spectrum Sensing

Spectrum sensing refers to the process of detecting and analyzing the presence or absence of signals in a given frequency band [30]. Fig. 3 illustrates an example sensing process. Spectrum perception changes dynamically over time due to variations in spectrum usage. At the time  $t_0$ , the idle resource blocks (RBs) are 2<sup>nd</sup> and 7<sup>th</sup>, our breathing movement sensing signals select the 2<sup>nd</sup> RB to be transmitted out. At the time  $t_1$ , signals will select the 5<sup>th</sup> to occupy. With this dynamic sensing process, the narrow sweep bandwidth mmWave FMCW signal

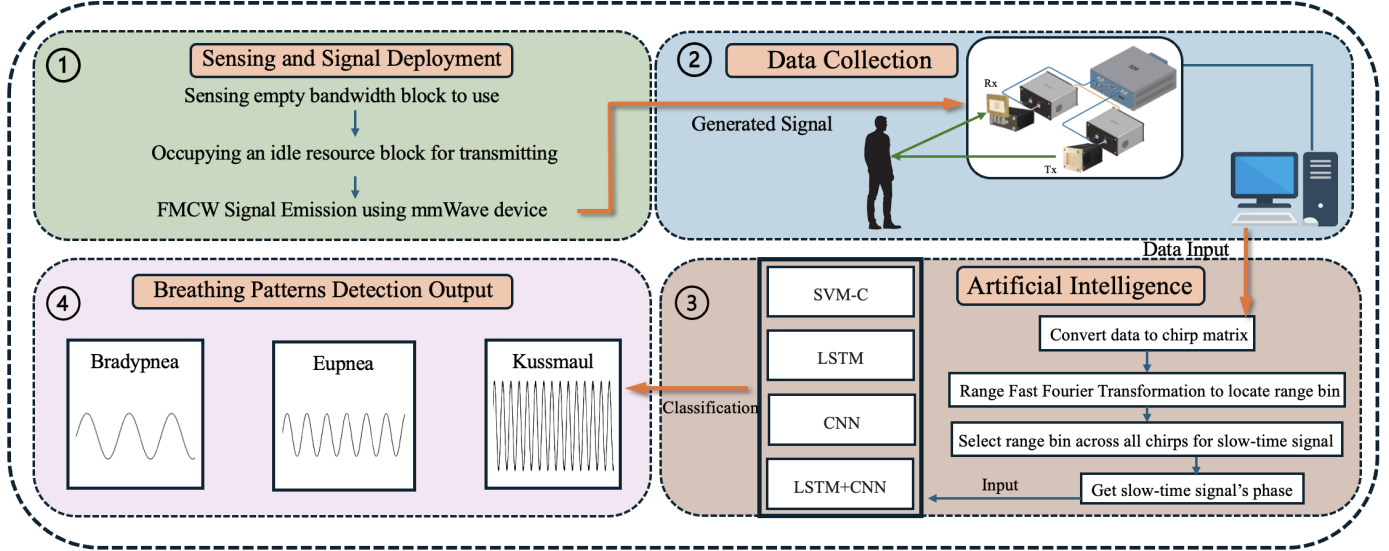


**Figure 4:** Design Overview. **Sensing and Signal Deployment:** Apply spectrum sensing, and select an idle RB to transmit the mmWave FMCW signal. **Data Collection:** Signal generated with a mmWave setup, and received signal data are collected on the server for further processing. **Artificial Intelligence:** Process the collected data, locate the subject, and apply artificial intelligence techniques (SVM-C, LSTM, CNN, and LSTM+CNN) for breathing patterns detection. **Breathing Patterns Detection Output:** Final classification results detect different breathing patterns: Bradypnea, Eupnea, and Kussmaul.

flexibly senses idle, fragmented resource blocks (RBs) over time to enable efficient signal transmission.

### B. Breathing Detection Scheme

With the basic idea of applying spectrum sensing to find fragmented bandwidth blocks for efficient resource utilization, we now investigate the detailed design of our breathing patterns detection scheme. Our scheme can be carried out with the following four steps as outlined in Fig. 4.

**1) Sensing and Signal Deployment:** The scheme first applies the spectrum sensing technique to sense idle RBs in the system for the FMCW signal transmitting.

**2) Data Collection:** The experiment testbed handles the initial of breathing data collection. It performs first step signal processing, including frequency difference calculation and fixed band filtering. This ensures that the processed data consists only of necessary information in signal components required for identifying breathing patterns.

**3) Artificial Intelligence:** The processed information from beat signal is used to locate our target in range profile and the signal component corresponding to the target over signal duration is extracted and is used to train machine learning and deep learning models illustrated in Section III-C for accurately distinguishing between the different breathing patterns.

**4) Breathing Patterns Detection Output:** The individual samples are classified according to the characteristics of each different pattern. Then, breathing patterns are detected successfully.

### C. Classification Mechanisms

The beat signal collected from the setup represents a sequential time-series data characterized by the signal's features

such as its magnitude, phase as well as the modulation induced by chest motion during respiration. While the magnitude represents the strength of the received signal, it is less sensitive to micro-displacements by respiration and is more prone to interference from external factors. The phase of the received signal is however highly sensitive to the modulations caused due to micro-displacements making it particularly effective in monitoring human vitals such as respiration rates. To classify these respiration patterns we used the machine learning and deep learning methods as shown in Fig. 5 and trained them on the phase values across the beat signal collected for 30 seconds. Each model is selected for its ability to handle the different aspects related to our data.

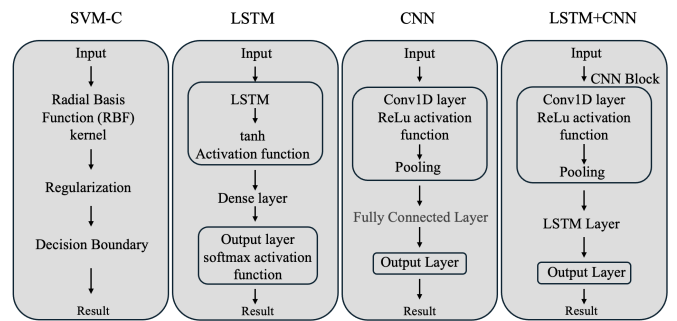


**Figure 5:** Classification Mechanisms of four machine learning models: SVM-C, LSTM, CNN, LSTM-CNN. These models are used for sequential data processing and classification.

**SVM-C:** Support Vector Machine is a traditional machine learning algorithm that finds an optimal hyperplane within the feature space of the data for effective classifications. While not inherently designed for sequential data, the SVM is compatible

to be trained on the phase values across our signal. The use of Radial Basis Function kernel allows SVM to effectively map phase values to a higher dimension space, allowing it to capture non-linear relationships, such as periodic respiration cycles and their frequency in different respiratory patterns and effectively classify them. While it does not directly model on the temporal dependencies it serves as a robust baseline for comparison with deep learning models.

**LSTM:** Long Short Term Memory (LSTM) networks are a enhancement over the Recurrent Neural Network (RNN) designed specifically to handle sequential data. They use a gating mechanism to selectively retain or discard information over time, allowing it to capture long-term relationships such as the periodic modulations due to respiration from our beat signal. The model trains on the sequential phase values, by analyzing the temporal structure of signal and retaining the subtle phase differences occurring over different cycles to distinguish between different patterns such as slow breaths in bradypnea, the regular breathing pattern of Eupnea or fast breaths in Kussmaul pattern effectively. Its ability to handle long sequences without losing the contextual information across the duration of signal makes it suitable for classification on our sequential data.

**CNN:** Convolutional Neural Network (CNN) is a deep learning model designed to extract spatial patterns and hierarchical features from data. Although commonly used for image processing CNNs have been proven effective for sequential 1-Dimensional data, such as the phase value sequences in beat signal, enabling it to capture localized features and trends. Its convolutional filters allow it to auto-extract the localized features and effectively analyze the spatial structure of the beat signal across time by identifying the repeating patterns in localized segments such as peaks and oscillations corresponding to a specific breathing pattern. CNNs weight-sharing mechanism between layers and auto-feature extraction makes it highly suitable for analyzing the raw or minimally processed beat signal data ensuring robust classification of different respiration patterns.

**LSTM+CNN:** The hybrid model combines the strengths of both the CNNs and LSTMs to fully leverage the spatial and temporal characteristics of beat signal. The first CNN layers focus on extracting the high-level spatial features corresponding to the respiration patterns by analyzing the phase changes in signal. While the LSTM layers capture the temporal dependencies such as frequency of respiration cycles modeling for the sequential nature of the data. By combining both the spatial feature extraction and establishing the temporal relationship, this model effectively tries to analyze for both local and global patterns within the beat signal to distinguish for different breathing patterns.

#### IV. EVALUATION

In this section, we experimentally validate the effectiveness of our breathing patterns detection.

**Experimental Setup:** As shown in Fig. 6a, a FMCW Radar system is implemented on NI-USRP (Universal Software

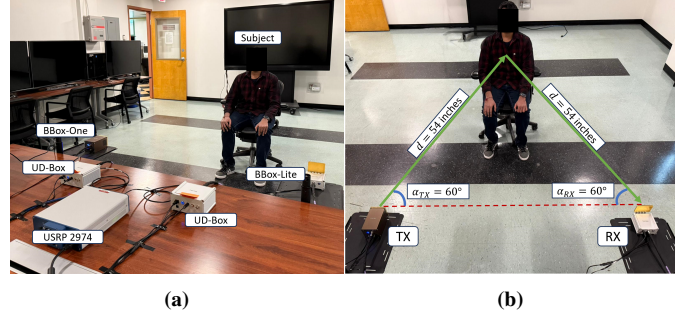


**Figure 6:** Breathing patterns detection experiment setup: (a) All participants in our experiment. (b) Specific antennas and subject setup for breathing patterns detection.

Radio Peripheral) 2974 using GNU-Radio software on the USRP's System on Module (SOM). The USRP generates and transmits FMCW signals at 2.8 GHz, which are connected to a mmWave beamforming development kit from TMYTEK. This kit includes a pair of Frequency Up/Down Converters (UD-Box) to upconvert the signals to 28 GHz for transmission. A 16-channel phased array antenna (BBox-One) is used to transmit the radar signals, while a 4-channel phased array antenna (BBox-Lite) is employed for receiving. Both antennas are configured at a 30 degree horizontal aperture to focus on a single human in line of sight, which means  $\alpha_{TX} = \alpha_{RX} = 60^\circ$  as shown in Fig. 6b.

The FMCW radar operates at a sample rate of 20 MHz with a 2 MHz sweep bandwidth, using a sawtooth waveform for modulation. The FMCW specifications are shown in the table II. The radar signal is transmitted on a single human

**Table II: FMCW RADAR SPECIFICATIONS**

PARAMETERS	VALUES
Sample Rate	20 MHz
Chirp Duration ( $T$ )	1 ms
Chirp Frequency	1 kHz
Sweep Bandwidth ( $B$ )	2 MHz
Range Resolution	75 m

in a line-of-sight at a distance  $d = 54$  inches (approximately 1.37 m), the reflected signal is de-chirped by mixing with the transmitted signal, decimated and resampled with a low-pass filter cutting off the higher frequency components. This reflected signal is collected from the subject whilst simulating one of the three types of patterns as described in Section II-B for 30 seconds, as it captures sufficient respiration cycles for differentiating each of the patterns and allowing for accurate analysis of its distinct periodic characteristics.

#### A. Respiration Detection

**Description of Dataset:** The collected beat signal is decimated and resampled with a low-pass filter, then organized into a chirp matrix, which provides range profiles for each of the transmitted chirp. The signal component then corresponding to the range bin of our target distance is extracted across all the range profiles. This extracted component represents our slow time signal over time which is used to track the

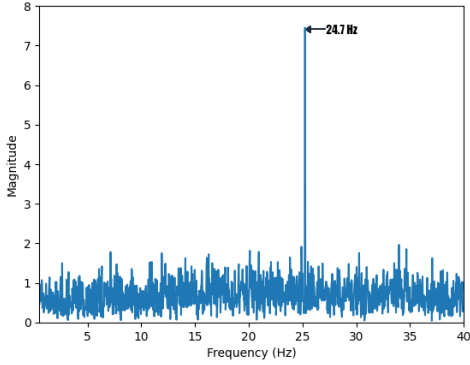


**Figure 7:** Range FFT for the beat single from a typical breathing sample

micro-displacements caused due to chest motion by analyzing its phase changes across the chirps. This slow time signal is extracted for various breathing frequencies under different respiratory patterns. For a total signal duration of 30 seconds and a chirp frequency of 1 kHz, the resulting slow time signal has a sequence length of 30,000 sample points corresponding to the component at the target range from each of the transmitted chirps. The phase values for these sequences are calculated for further analysis, including the detection of respiratory rate and training the machine learning and deep learning models for classifying the different respiratory patterns.

Breathing typically modulates the reflected signal by a few millimeters at a frequency of around 0.2-0.5 Hz (12-30 breaths/min). These modulations do not appear in fast-time Range FFT but periodically within the same range bin over time. To identify these modulations caused by respiration, we first calculate the Range FFT across the beat signal to identify the beat frequency peaks to locate our target as shown by the Range FFT plot in Fig. 7, the peak at 24.7 Hz indicates the distance to target at 1.87m indicating an error of about 50cm from our true distance. The range bin of this peak is selected and the slow time signal at this bin is extracted across all the chirps. A Slow Time FFT is applied across this signal to get the peak frequency within the 0.1-0.5 Hz range which forms our breath frequency. The detected respiration rates captured under Bradypnea pattern are shown in Fig. 8a with rate of 3-4 breaths range for 30 seconds, Fig. 8b captures range of 7-10 breaths under Eupnea condition and the fast breaths captured under Kussmaul pattern are shown in Fig. 8c capturing respiration rates of 11-14 breaths for 30 seconds.

**Table III: CLASSIFICATION ACCURACY**

METHOD	ACCURACY
SVM-C	83%
LSTM	80%
CNN	90%
CNN + LSTM	77%

### B. Machine Learning

With the beat signal analysis we are able to accurately detect the respiration rate, but detecting the respiratory pattern based

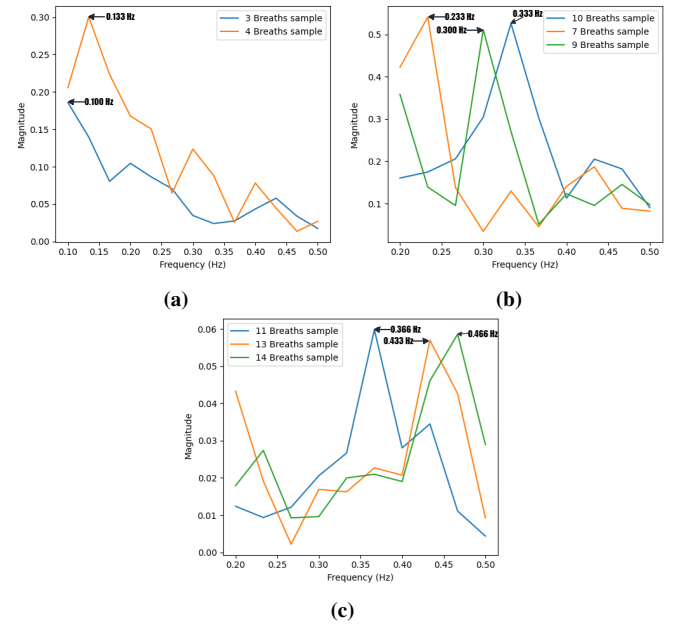


**Figure 8:** Respiratory rate identify. (a) Bradypnea. (b) Eupnea. (c) Kussmaul.

only on it may not always be accurate due to overlaps in ranges of respiratory rate in different types of patterns. So to more accurately classify our breathing samples into different types we utilized machine learning and deep learning models described in III-C. These models are trained on the phase values of slow time signal to detect for different patterns shown in Fig. 2.

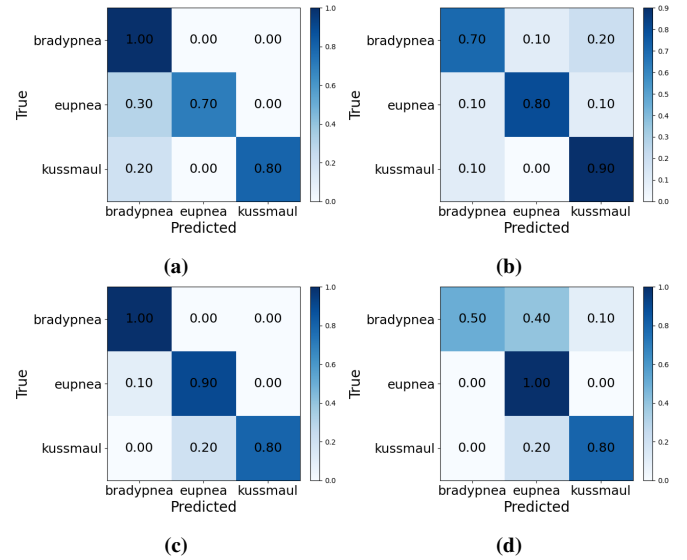


**Figure 9:** Confusion matrix for different classification mechanisms. (a) SVM-C. (b) LSTM. (c) CNN. (d) LSTM+CNN.

The classification results for different methods are shown in Fig. 9. The traditional SVM Classification showed 83% accuracy overall, demonstrating its capability as a baseline approach. While the miss-classifications showed overfitting towards Bradypnea Type. The LSTM model designed to

handle our sequential data shows an accuracy of 80%, this model effectively classified Kussmaul and Eupnea samples, and with further optimizations performance for Bradypnea samples samples can be improved. The CNN model achieves the highest overall accuracy of 90%, showcasing its robust performance in capturing the periodic patterns of different respiration patterns in beat signal. To capture the periodic moments more accurately over the sequential data the LSTM model is used in combination with CNN layers however this showed an decrease in performance achieving only 77% accuracy indicating opportunities to further optimize the model structure to fully utilize the combined strengths of both methods.

## V. CONCLUSION

In this paper, we address the challenge of contactless breathing pattern classification and detection. Different from previous solutions, our design enables breathing pattern detection using fragmented sweep bandwidth in resource-constrained systems. By leveraging FMCW mmWave radar sensing at 28 GHz with a constrained bandwidth of 2 MHz, our approach meets both communication and sensing requirements for in-home health monitoring applications, eliminating the need for additional hardware beyond standard communication devices. Experimental validation on a USRP platform demonstrates the effectiveness of our design. Using machine learning algorithms—SVM-C, LSTM, CNN, and LSTM+CNN—to classify extracted features. The CNN classifier performed the best out of the four models, with an overall accuracy rate of 90%.

## REFERENCES

- [1] Stock M. C. Capnography for adults, 1995. <https://pubmed.ncbi.nlm.nih.gov/7736268/>.
- [2] A Jubran. Pulse oximetry. *Crit. Care*, 3(2):R11–R17, 1999.
- [3] A J Williams. ABC of oxygen: assessing and interpreting arterial blood gases and acid-base balance. *BMJ*, 317(7167):1213–1216, October 1998.
- [4] Jürgen Biederer, S Mirsadraee, M Beer, F Molinari, C Hintze, G Bauerman, M Both, E J R Van Beek, J Wild, and M Puderbach. MRI of the lung (3/3)-current applications and future perspectives. *Insights Imaging*, 3(4):373–386, August 2012.
- [5] Yann Retory, Pauline Niedzialkowski, Carole de Picciotto, Marcel Bonay, and Michel Petitjean. New respiratory inductive plethysmography (RIP) method for evaluating ventilatory adaptation during mild physical activities. *PLoS One*, 11(3):e0151983, March 2016.
- [6] K. S. Tan, R. Saatchi, H. Elphick, and D. Burke. Real-time vision based respiration monitoring system. In *2010 7th International Symposium on Communication Systems, Networks & Digital Signal Processing (CSNDSP 2010)*, pages 770–774, 2010. doi: 10.1109/CSNDSP16145.2010.5580316.
- [7] Supriya Sathyaranayana, Ravi Kumar Satzoda, Suchitra Sathyaranayana, and Srikanthan Thambipillai. Vision-based patient monitoring: a comprehensive review of algorithms and technologies. *J. Ambient Intell. Humaniz. Comput.*, 9(2):225–251, April 2018.
- [8] Integrated sensing and communication emerging technology initiative. <https://isac.committees.comsoc.org/>.
- [9] Jian Liu, Yingying Chen, Yan Wang, Xu Chen, Jerry Cheng, and Jie Yang. Monitoring vital signs and postures during sleep using wifi signals. *IEEE Internet of Things Journal*, 5(3):2071–2084, 2018. doi: 10.1109/JIOT.2018.2822818.
- [10] Jiefan Qiu, Pan Zheng, Kaikai Chi, Ruiji Xu, and Jiajia Liu. Respiration monitoring in high-dynamic environments via combining multiple wifi channels based on wire direct connection between rx/tx. *IEEE Internet of Things Journal*, 10(2):1558–1573, 2023. doi: 10.1109/JIOT.2022.3209172.
- [11] Chaowei Zang, Chi Zhang, Min Zhang, and Qiang Niu. An RFID-based method for multi-person respiratory monitoring. *Sensors (Basel)*, 22(16):6166, August 2022.
- [12] Lili Chen, Jie Xiong, Xiaojiang Chen, Sunghoon Ivan Lee, Daqing Zhang, Tao Yan, and Dingyi Fang. Lungtrack: Towards contactless and zero dead-zone respiration monitoring with commodity rfids. *Proc. ACM Interact. Mob. Wearable Ubiquitous Technol.*, 3(3), September 2019. doi: 10.1145/3351237. URL <https://doi.org/10.1145/3351237>.
- [13] Changzhi Li, Victor M. Lubecke, Olga Boric-Lubecke, and Jenshan Lin. A review on recent advances in doppler radar sensors for noncontact healthcare monitoring. *IEEE Transactions on Microwave Theory and Techniques*, 61(5):2046–2060, 2013. doi: 10.1109/TMTT.2013.2256924.
- [14] Dongyu Miao, Heng Zhao, Hong Hong, Xiaohua Zhu, and Changzhi Li. Doppler radar-based human breathing patterns classification using support vector machine. In *2017 IEEE Radar Conference (RadarConf)*, pages 0456–0459, 2017. doi: 10.1109/RADAR.2017.7944246.
- [15] A. Droitcour, V. Lubecke, Jenshan Lin, and O. Boric-Lubecke. A microwave radio for doppler radar sensing of vital signs. In *2001 IEEE MTT-S International Microwave Symposium Digest (Cat. No.01CH37157)*, volume 1, pages 175–178 vol.1, 2001. doi: 10.1109/MWSYM.2001.966866.
- [16] Chi-Hsuan Hsieh, Yu-Fang Chiu, Yi-Hsiang Shen, Ta-Shun Chu, and Yuan-Hao Huang. A uwb radar signal processing platform for real-time human respiratory feature extraction based on four-segment linear waveform model. *IEEE Transactions on Biomedical Circuits and Systems*, 10(1):219–230, 2016. doi: 10.1109/TBCAS.2014.2376956.
- [17] Siying Wang, Antje Pohl, Timo Jaeschke, Michael Czaplik, Marcus Köny, Steffen Leonhardt, and Nils Pohl. A novel ultra-wideband 80 ghz fmcw radar system for contactless monitoring of vital signs. In *2015 37th Annual International Conference of the IEEE Engineering in Medicine and Biology Society (EMBC)*, pages 4978–4981, 2015. doi: 10.1109/EMBC.2015.7319509.
- [18] K van Loon, M J M Breteler, L van Wolfwinkel, A T Rheineck Leyssius, S Kossen, C J Kalkman, B van Zaane, and L M Peelen. Wireless non-invasive continuous respiratory monitoring with FMCW radar: a clinical validation study. *J. Clin. Monit. Comput.*, 30(6):797–805, December 2016.
- [19] Mi He, Yongjian Nian, and Yushun Gong. Novel signal processing method for vital sign monitoring using fmcw radar. *Biomedical Signal Processing and Control*, 33:335–345, 2017. ISSN 1746-8094. doi: <https://doi.org/10.1016/j.bspc.2016.12.008>. URL <https://www.sciencedirect.com/science/article/pii/S1746809416302208>.
- [20] Arnau Prat, Sebastián Blanch, Albert Aguasca, Jordi Romeu, and Antoni Broquetas. Collimated beam fmcw radar for vital sign patient monitoring. *IEEE Transactions on Antennas and Propagation*, 67(8): 5073–5080, 2019. doi: 10.1109/TAP.2018.2889595.
- [21] Mostafa Alizadeh, George Shaker, João Carlos Martins De Almeida, Plínio Pelegrini Morita, and Safeddin Safavi-Naeini. Remote monitoring of human vital signs using mm-wave fmcw radar. *IEEE Access*, 7: 54958–54968, 2019. doi: 10.1109/ACCESS.2019.2912956.
- [22] Gen Li, Yun Ge, Yiyu Wang, Qingwu Chen, and Gang Wang. Detection of human breathing in non-line-of-sight region by using mmwave fmcw radar. *IEEE Transactions on Instrumentation and Measurement*, 71: 1–11, 2022. doi: 10.1109/TIM.2022.3208266.
- [23] Yong Wang, Wen Wang, Mu Zhou, Aihu Ren, and Zengshan Tian. Remote monitoring of human vital signs based on 77-ghz mm-wave fmcw radar. *Sensors*, 20(10), 2020. ISSN 1424-8220. doi: 10.3390/s20102999. URL <https://www.mdpi.com/1424-8220/20/10/2999>.
- [24] Zhanjun Hao, Yue Wang, Fenfang Li, Guozhen Ding, and Yifei Gao. mmwave-rm: A respiration monitoring and pattern classification system based on mmwave radar. *Sensors*, 24(13), 2024. ISSN 1424-8220. doi: 10.3390/s24134315. URL <https://www.mdpi.com/1424-8220/24/13/4315>.
- [25] Qisong Wang, Zhening Dong, Dan Liu, Tianao Cao, Meiyang Zhang, Runqiao Liu, Xiaocong Zhong, and Jinwei Sun. Frequency-modulated continuous wave radar respiratory pattern detection technology based on multifeature. *J. Healthc. Eng.*, 2021:9376662, August 2021.
- [26] Whited L, Hashmi MF, and Graham DD. *Abnormal Respirations*. [Updated 2023 Nov 5], In StatPearls [Internet], 2024. <https://www.ncbi.nlm.nih.gov/books/NBK470309/>.
- [27] Dong S, and Wen L, and Li Y. Remote respiratory variables tracking with biomedical radar-based iot system during sleep. *IEEE Internet of Things Journal*, 11:19937–19948, 2024. <https://ieeexplore.ieee.org/document/10440444>.

- [28] J. Kunczik, K. Hubermann, and L. Mösch. Breathing pattern monitoring by using remote sensors. *Sensors*, 22(8854):1–21, 2022. <https://www.mdpi.com/1424-8220/22/22/8854>.
- [29] Zhai Q.and Han X.and Han Y.and Yi J. A contactless on-bed radar system for human respiration monitoring. *IEEE Transactions on Instrumentation and Measurement*, 71:1–10, 2022. <https://ieeexplore.ieee.org/document/9749062>.
- [30] Youness Arjoune and Naima Kaabouch. A comprehensive survey on spectrum sensing in cognitive radio networks: Recent advances, new challenges, and future research directions. *Sensors*, 19(1), 2019. ISSN 1424-8220. doi: 10.3390/s19010126. URL <https://www.mdpi.com/1424-8220/19/1/126>.